



## Supplementary Materials for

### **Homer1a Drives Homeostatic Scaling-down of Excitatory Synapses During Sleep**

Graham H. Diering, Raja S. Nirujogi, Richard H. Roth, Paul F. Worley, Akhilesh Pandey,  
Richard L. Huganir\*

\*correspondence to: [rhuganir@jhmi.edu](mailto:rhuganir@jhmi.edu)

#### **This PDF file includes:**

Materials and Methods  
Figs. S1 to S8  
Tables S1 and S2  
Full Reference List

## **Materials and Methods**

### Animal use and tissue collection

All animals were treated in accordance with the Johns Hopkins University Animal Care and Use Committee guidelines. For all experiments animals were kept on a 12hr:12hr light/dark cycle with lights on at 6am and lights off at 6pm. For all experiments mice were age 8-10 weeks and were group housed with 3-4 individuals per cage. For pharmacology experiments mice were treated with drugs via intraperitoneal (IP) injection. For biochemistry experiments mice were collected at either 10am or 10pm, anesthetized by inhalation of isoflurane for 15sec followed immediately by cervical dislocation, brains were removed and forebrains (cerebral cortex plus hippocampus) were dissected in ice-cold PBS and immediately frozen on dry ice. Samples were kept at -80°C until used for sub-cellular fractionation.

### Sleep Deprivation and Video Monitoring

For sleep deprivation experiments mice were placed individually in a clean standard mouse cage at the beginning of the light phase (6am) and remained there for 4hrs (10am). Towards the end of this period mice were additionally stimulated by gentle tapping of the cage or by disturbing the bedding material. Mice were then sacrificed for tissue collection or returned to their original cage with their original cage mates for recovery sleep and left undisturbed for an additional 2.5hrs (12:30pm) followed by sacrifice. As a control, mice that were undisturbed were collected 4hrs into the light phase (10am). In some experiments mice received an injection at the onset of sleep deprivation and again 2hrs later. For video monitoring of sleep, undisturbed mice were continually recorded with a standard video recorder through the light dark cycle. A red lamp was used for illumination during the dark phase. Sleep and wake activity was scored manually during the first 4hrs of the light or dark phase. Data are presented as percent total time spent awake.

### Neuron culture

Cortical neurons obtained from Sprague-Dawley rats at embryonic day 18 were plated onto poly-L-lysine coated standard 6-well tissue culture dishes at a density of 600,000 cells/well and grown in glia-conditioned neurobasal media supplemented with 2% B-27, 2mM Glutamax, 50U/mL PenStrep, and 1% horse serum. Cultured neurons were fed twice per week. Cortical neurons (grown for 13-14 days *in vitro*) were treated for 24hrs with bicuculline methobromide (20 $\mu$ M) to induce homeostatic scaling-down. In some experiments, following bicuculline treatment neurons were treated with DHPG (100 $\mu$ M) for 5-10min or noradrenaline (5 $\mu$ M) for 1hr. In some experiments neurons were treated for 30min with adenosine (10 $\mu$ M) dissolved in water or CCPA (100nM) dissolved in DMSO. Neurons were then lysed in lysis buffer (PBS containing 50mM NaF, 5mM sodium pyrophosphate, 1% triton X-100, 0.5% sodium deoxycholate, 0.02% SDS, 200nM okadaic acid, 1mM Na<sub>3</sub>VO<sub>4</sub>, and protease inhibitor cocktail), or homogenized in homogenization buffer (320mM sucrose, 5mM sodium pyrophosphate, 1mM EDTA, 10mM HEPES pH 7.4, 200nM okadaic acid, protease inhibitor cocktail), followed by sub-cellular fractionation.

### Antibodies

The following mouse monoclonal primary antibodies were used: anti-GluA1 N-terminal antibody (4.9D, made in house), anti-GluA2 N-terminal antibody (032.19.9, made in house), anti-GluA2 phospho-S880 specific (02.22.4, made in house), anti-PSD95, pan-Shank and IP3R (NeuroMab), anti-phospho-ERK1/2 (Cell Signaling Technologies). The following rabbit primary antibodies were used: anti-GluN1, GluN2B, GluN2A (made in house), anti-GluA1 phospho-S845 specific and anti phospho-S831 specific (Millipore), anti-GluA3 (JH4300, made in house), anti-PKA catalytic subunit, PKC $\gamma$ , mGluR5 (AbCam), anti-AKAP5 (BD biosciences), anti-ERK1/2 (Cell Signaling Technologies), anti-Homer1 (long) and anti-Homer1a (Synaptic Systems). The following additional antibodies were used: IRDye650-conjugated goat anti-mouse and IRDye800-conjugated goat anti-rabbit (Li-Cor), horseradish peroxidase-conjugated anti-rabbit and anti-mouse (Thermo), and horseradish peroxidase-conjugated goat anti-mouse and mouse anti-rabbit light chain specific (Jackson).

#### Drugs and treatments

MTEP hydrochloride (2.5mg/mL in PBS containing 5% TWEEN 80), JNJ16259685 (1.25mg/mL in PBS containing 5% TWEEN 80), D-Amphetamine sulfate (4mg/mL in PBS), prazosin (4mg/mL in PBS), propranolol (40mg/mL in PBS), DPCPX (1mg/mL in PBS containing 5% DMSO), bicuculline methochloride (20mM in water), D/L-DHPG (10mM in water), and CCPA (1mM in DMSO) were purchased from Tocris. Adenosine (10mM in water) was purchased from Sigma. MTEP and JNJ16259685 were injected as a cocktail (5mg/kg and 2.5mg/kg respectively) either following contextual fear conditioning or 2hrs prior to brain collection and sub-cellular fractionation. D-Amphetamine sulfate was injected at 2mg/kg and brains were collected and processed 2hrs later. Prazosin and propranolol were injected as a cocktail (2mg/kg and 20mg/kg respectively) and brains were collected 2hrs later. DPCPX was injected at 0.5mg/kg at the onset of sleep deprivation and again 2hrs later.

#### Contextual fear conditioning

Mice were handled gently for 5min/day for 3 consecutive days prior to each experiment. On the day of training, at either 8am or 6pm, mice were allowed to explore the conditioning chamber for 4min prior to a 2sec 0.3mA foot-shock. Animals were left in the chamber for an additional 2min following the shock and then returned to their home cage. The training chamber was scented with ethanol. 20-30min following contextual fear conditioning animals received an injection of vehicle (PBS/5% TWEEN 80) or MTEP (5mg/kg)/JNJ16259685 (2.5mg/kg) cocktail. 24 or 36hrs post-training, in order to test mice at the same time of day, mice were returned to the training chamber for 2min and freezing responses were measured. 6hrs later, mice were placed in a novel context, scented with acetate, for 2min, in which they did not receive a foot-shock and freezing was assessed. Freezing responses were analyzed using automated tracking software and expressed as a percentage of total time spent on the testing chamber.

#### PSD prep

*Mouse forebrain:* Frozen forebrains (cortex plus hippocampus) were homogenized using 12 strokes from a glass homogenizer in ice-cold homogenization solution (320mM sucrose, 10mM HEPES pH 7.4, 1mM EDTA, 5mM Na pyrophosphate, 1mM Na<sub>3</sub>VO<sub>4</sub>,

200nM okadaic acid, protease inhibitor cocktail). Brain homogenate was then centrifuged at 800xg for 10min at 4°C to obtain the P1 (nuclear) and S1 (post-nuclear) fractions. The S1 fraction was then subjected to centrifugation at 16,000xg for 20min at 4°C to obtain the P2 (membrane) and S2 (cytosol) fractions. The P2 fraction was resuspended in homogenization buffer, layered on top of a discontinuous sucrose density gradient (0.8M, 1.0M or 1.2M sucrose in 10mM HEPES pH 7.4, 1mM EDTA, 5mM Na pyrophosphate, 1mM Na<sub>3</sub>VO<sub>4</sub>, 200nM okadaic acid, protease inhibitor cocktail) and then subjected to ultra-centrifugation at 82,500xg for 2hr at 4°C. Material accumulated at the interface of 1.0M and 1.2M sucrose (synaptosomes) was collected. Synaptosomes were diluted using 10mM HEPES pH7.4 (containing protease and phosphatase inhibitors) to restore the sucrose concentration back to 320mM. The diluted synaptosomes were then pelleted by centrifugation at 100,000xg for 30min at 4°C. The synaptosome pellet was then resuspended in 50mM HEPES pH 7.4 and then mixed with an equal part 1% Triton X-100 (both solutions contained protease and phosphatase inhibitors). This mixture was incubated at 4°C with rotation for 15min followed by centrifugation at 32,000xg for 20min to yield the post-synaptic density (PSD) preparation. The PSD material was then resuspended in 50mM HEPES pH 7.4 (plus protease and phosphatase inhibitors). The protein concentration was determined using Bradford assay and material was analyzed by Western blot.

*Cultured neurons:* Cells were collected by scraping and homogenized by passage through a 26g needle, 12 times, in homogenization buffer (320mM sucrose, 5mM sodium pyrophosphate, 1mM EDTA, 10mM HEPES pH 7.4, 200nM okadaic acid, protease inhibitor cocktail). The homogenate was centrifuged at 800xg for 10min at 4°C to yield P1 and S1. S1 was further centrifuged at 15,000xg for 20min at 4°C to yield P2 and S2. P2 was resuspended in milliQ water, adjusted to 4mM HEPES pH 7.4 from a 1M HEPES stock solution, and incubated with agitation at 4°C for 30min. The suspended P2 was centrifuged at 25,000xg for 20min at 4°C to yield LP1 and LS2. LP1 was resuspended in 50mM HEPES pH 7.4, mixed with an equal volume of 1% triton X-100, and incubated with agitation at 4°C for 15min. The PSD was generated by centrifugation at 32,000xg for 20min at 4°C. The final PSD pellet was resuspended in 50mM HEPES pH 7.4 followed by protein quantification and Western blot.

#### Co-immunoprecipitation

P2 fractions were prepared as above for mouse forebrain (10pm or 10am) or cortical neurons (13DIV) treated with bicuculline for 24hrs. P2 fractions were lysed in PBS containing 50mM NaF, 5mM sodium pyrophosphate, 1% triton X-100, 0.5% sodium deoxycholate, 0.02% SDS, 200nM okadaic acid, 1mM Na<sub>3</sub>VO<sub>4</sub>, and protease inhibitor cocktail, and P2 lysates were cleared by centrifugation at 16,000xg for 20min at 4°C. Protein concentration of the P2 lysate was determined using Bradford assay and 250µg of protein was incubated overnight with 0.2µL of rabbit anti-Homer1L antibody and 20µL protein A sepharose beads, or 1µL of mouse anti-IP3R antibody and 20µL protein G sepharose beads. P2 lysate incubated with protein A or G beads without antibody was used as a control. Beads were then washed 5 times with lysis buffer and protein was eluted using 2xSDS-sample buffer. 5µg of lysate was included as an input control. Samples were analyzed by Western blot using HRP-conjugated light chain specific secondary antibodies.

### In vivo two-photon imaging

Cortical layer V neurons in the mouse motor cortex were transfected with SEP-GluA1, myc-GluA2, and dsRed2 by targeted *in utero* electroporation in E13 embryos as previously described(13, 32). GluA1 tagged with a pH-sensitive form of GFP (Super Ecliptic pHluorin (SEP)) specifically visualizes surface inserted GluA1, GluA2 was included to approximate the natural GluA1/GluA2 ratio in transfected neurons, dsRed2 serves as a morphology marker for transfected neurons.

At the age of 8-10 weeks a 3x3mm cranial window was placed over the motor cortex(13). The window was centered using stereotactic coordinates 2mm lateral of bregma. Mice were anesthetized using Avertin and the skull was sealed using dental cement. A metal head bar was attached to the skull during surgery to fixate the mouse during imaging. Mice were housed individually after surgery and allowed to recover for 2-3 weeks before imaging.

*In vivo* images were acquired of mice under isoflurane anesthesia (1.5-2% vol isoflurane/vol O<sub>2</sub>) with a custom-built, two-photon laser-scanning microscope controlled by ScanImage written in MATLAB(33). Mice were habituated to handling and anesthesia for three days before the beginning of imaging and subsequently imaged twice a day at 10am and 10pm over the course of three days. Apical dendrites of layer V pyramidal neurons were imaged using a 20x/1.0 NA water-immersion objective lens. SEP-GluA1 and dsRed2 were excited at 910 nm with a Ti:sapphire laser with ~100 mW of power delivered to the back-aperture of the objective. Image stacks were acquired at 1,024 × 1,024 pixels with a voxel size of 0.12 μm in x and y and a z-step of 1 μm. Representative images shown in figures were median filtered, up-scaled, and contrast enhanced.

### Analysis of *in vivo* images

Signal intensity in spines was analyzed using a custom-written software in Igor Pro as previously described(13). In brief, three dimensional ROIs were defined for each spine, the dendritic shaft adjacent to that spine, and a nearby background region. To compare intensity values between imaging sessions, the spine SEP-GluA1 or spine dsRed signal was normalized to the dsRed signal on the adjacent dendritic shaft after background subtraction. To account for differences in SEP-GluA1 and dsRed expression levels between different neurons and animals, spine SEP-GluA1 or spine dsRed signal was further normalized to the average spine SEP-GluA1 or spine dsRed signal of all PM time points. Only spines that were existent in at least 4 imaging sessions were included in the analysis. For data analysis and representation spine intensity values at all PM time points and all AM time points were averaged.

### Sample preparation for proteomic and phosphoproteomic analysis

PSD preps from five mice from each 10pm and 10am condition were pooled, homogenized in lysis buffer (2% SDS, 50mM TEABC) and sonicated for 30 seconds. The protein lysate was clarified by centrifuging at 16,000g for 15min at room temperature. Protein estimation was carried out using BCA assay and 1mg from each 10pm and 10am condition was subjected for proteomic sample preparation. Protein was reduced with 10mM DTT and incubated at 56<sup>0</sup>C for 20min followed by alkylation with 20mM IAA for 30min at room temperature in the dark. Filter assisted sample preparation

(FASP) was used(34) to clear the SDS by buffer exchange with 9M Urea buffer using 30kDa *cut-off* filters and centrifuged at 14,000g for 15min. Three rounds of such cycles were repeated followed by two rounds of buffer exchange with 50mM TEABC. The final retentate was collected in 50mM TEABC buffer and subjected to trypsin digestion. Trypsin was added at 1:50 (enzyme to substrate) ratio and was incubated overnight at 37°C. Trypsin activity was quenched by adding 1% TFA and the tryptic digest from both the conditions were desalted using C<sub>18</sub> cartridges. Eluted peptides were vacuum dried and stored in -80°C deep freezer until further analysis.

#### Tandem mass tags (TMT) labeling

The desalted peptides were dissolved in 50mM TEABC buffer (pH 8.0). Peptide amount was measured using peptide colorimetric assay to ensure equal amount for peptide amount for TMT labeling in each condition. To avoid the instrumental technical bias 1 mg peptide amount was split into two equal amounts from each condition, 10am and 10pm for 4 plex TMT labeling as technical replicates. TMT reporter tags 126/128 and 130/131 from 6 plex TMT labeling kit were labeled for 10am and 10pm respectively. TMT labeling was carried out as per manufacturer instructions. TMT reagents were equilibrated to room temperature followed by addition of 41µl of anhydrous acetonitrile. Peptide amount from each condition (500µg per condition) was added to the corresponding TMT reporter tag, briefly vortexed and incubated at room temperature for 1hr. To ensure the complete labeling 1 to 2µg from each channel were mixed, desalted and analyzed on Orbitrap Fusion mass spectrometer (during this individual labeled sample was kept at 4°C). The reaction was further quenched by adding 1% hydroxyl amine, further all channel were pooled and vacuum dried.

#### Basic reverse-phased liquid chromatography (bRPLC) fractionation

The TMT labeled and pooled peptide digest was dissolved in bRPLC solvent A (10mM TEABC). Sample was fractionated on an offline fractionation HPLC system which consists of a binary pump, VWD detector and a fraction collector. Sample was fractionated by applying a linear gradient of 3% to 60% solvent B (10mM TEABC in 90% ACN) at a flow rate of 0.5 ml/min on an Xbridge bRPLC column. The VWD detector was operated at 280nm. The loading, gradient includes a 130min run time and a total of 96 fraction were collected. 96 fractions were concatenated to 12 fractions for final TiO<sub>2</sub>-based phosphopeptide and global proteomic analysis. 1/10<sup>th</sup> of peptide amount from each fraction was separated and vacuum dried separately for global proteomic analysis and the remainder was vacuum dried for TiO<sub>2</sub> enrichment.

#### Titanium dioxide (TiO<sub>2</sub>)-based phosphopeptide enrichment

Each fraction was enriched for phosphopeptides using the TiO<sub>2</sub> strategy. Titansphere (5µm) beads were equilibrated using 5% DHB (dihydroxy benzoic acid) solution at room temperature. The dried peptides were reconstituted in 100µl DHB solution. The 1:1 ratio of titansphere bead to peptide amount was added and incubated for one hour at room temperature on a rotator. Further, each fraction was washed using 400µl of wash buffer (80% ACN in 4% TFA) and centrifuged at 1,500g for 1min. After 2 wash cycles the bead solution was loaded on C8 stage-tip plugs. The enriched phosphopeptides were eluted by adding 4% NH<sub>4</sub>OH solution directly into 1.5ml Eppendorff tubes containing 40µl of 4%

TFA solution on ice. The eluted peptides were vacuum dried and desalted using C<sub>18</sub> stage-tips(34) and stored in -80°C deep freezer until the LC-MS/MS analysis.

#### LC-MS/MS analysis

Total PSD peptide or enriched phosphopeptide fractions were analyzed with an Orbitrap Fusion mass spectrometer coupled to Easy nano LC 1000 UHPLC system. The peptides were dissolved in 0.1% FA and loaded on a trap column (2µm, 100Å, 100 µ ID. C<sub>18</sub>, 2cm, ES 801) and resolved on 50cm analytical column (2µm, 100Å, 75 µ ID. C<sub>18</sub>, 50cm ES 803,) using Easy nanospray source. The peptides were resolved by applying a linear gradient of 8% to 32% over 90min at a flow rate of 250nl/min. The total run time was 120min for each fraction. The Orbitrap Fusion mass spectrometer was operated in a data dependent MS<sup>2</sup> mode at High-High Orbitrap mode. The full scans in the range of m/z 350-1500 was separated using Quadrupole mass filter with 2 m/z isolation width and 0.6 m/z isolation off set and were measured using an Orbitrap mass analyzer at a mass resolution of 120,000 at m/z 200. The data was acquired in top speed for 3 seconds includes both survey and product ion scans. The MS<sup>2</sup> scans were acquired in Orbitrap mass analyzer at 30,000 resolution at m/z 200 and the precursor ions were fragmented using higher energy collisional dissociation (HCD) at 37% normalized collision energy. The ion filling times and AGC targets were set at 60ms and 1X10<sup>6</sup> for full scans and 5X10<sup>4</sup> and 100ms for MS<sup>2</sup> scans respectively. Dynamic exclusion was enabled and repeat duration was set for 45sec. Isobaric mass tag m/z 230.14 (TMT) was excluded for MS<sup>3</sup> mode. Internal calibration was carried out using lock mass option (m/z 445.1200025)(35) from ambient air. For the global proteomic analysis, each bRPLC fraction was analyzed on a mass spectrometer interfaced with a liquid chromatography system. The dissolved peptides were loaded on a pre-column and resolved on a 50cm analytical column. The peptides were resolved by applying a linear gradient of 8% to 32% solvent B (0.1% FA in 95% ACN) for 90min at flow rate of 250nl/min. The total run time included 120min. The Orbitrap Fusion Lumos mass spectrometer was operated in a data dependent MS<sup>3</sup> mode at High-High-High Orbitrap mode. The full scans in the range of m/z 350-1500 was separated using Quadrupole mass filter with 2 m/z isolation width and 0.6 m/z isolation off set and were measured using a mass analyzer at a mass resolution of 120,000 at m/z 200. The data was acquired in top speed for 3sec includes both survey and product ion scans. The MS<sup>2</sup> scans were acquired at 30,000 resolution at m/z 200 and the precursor ions were fragmented using higher energy collisional dissociation (HCD) at 37% normalized collision energy. The synchronous precursor selection was enabled to select top 10 product ions from MS<sup>2</sup> scan and were fragmented using higher energy collisional dissociation (HCD) at 55% normalized collision energy. The ion filling times and AGC targets were set at 60ms and 1X10<sup>6</sup> for full scans and 5X10<sup>4</sup> and 100ms for MS<sup>2</sup> and MS<sup>3</sup> scans respectively. Dynamic exclusion was enabled and repeat duration was set for 45sec. Isobaric mass tag m/z 230.14 (TMT) was excluded for MS<sup>3</sup> mode. Internal calibration was carried out using lock mass option (m/z 445.1200025)(35).

#### Mass spectrometry data analysis

The mass spectrometry raw files that are acquired as technical runs were used for the peptide and protein identification and quantification. The raw data was processed through

a software suite to generate peak list files for the database searches. Combined Sequest and Mascot search algorithms were used for the peptide identification and reporter ion quantifier node was enabled for peptide quantification and was searched against mouse Refseq 73 protein database. A dual workflow processing and consensus workflows were created with the following parameters. a) Minimum and maximum precursor were selected as 350Da and 8000Da respectively; b) Trypsin is selected as protease and a maximum of 2 missed cleavages were allowed; c) Precursor and fragment mass tolerance were set as 20 ppm and 0.1Da respectively; d) Oxidation of methionine residue as static modification and Carbamidomethylation of cysteine, phosphorylation of Ser, Thr and Tyr residues, peptide N-terminus and lysine side chain as TMT reported tag were selected as variable modification. Percolator node was used for calculating p value of identified PSMs and peptides for statistical significance. 1% protein level and peptide level FDR was used in the consensus workflow. The peptide quantification was carried out using reporter ion quantifier and isolation interference cut-off was set as 30% in order to account for the interference from co-eluting peptides. Only peptides falling below this criterion was considered for peptide quantification. For the global proteomic analysis the reporter ion quantification was enabled as MS3 such that the quantification values for the identified peptide precursors will be used for MS3 scans.

### Statistics

For biochemistry experiments comparing wake to sleep phases or contextual fear conditioning data, unpaired two-sided Student's t-test was used. When needed, t-tests were corrected for multiple comparisons using the Bonferroni correction, for example in experiments examining the effect of sleep deprivation and recovery. In all experiments, sleep was compared to wake, or treatment was compared to control. For *in vivo* imaging data paired two-sided t-tests were used for data presented in bar graph, for data presented as a histogram the Kolmogorov-Smirnov test was used. N values are indicated in the figure legends. All error bars represent standard error of the mean (SEM).



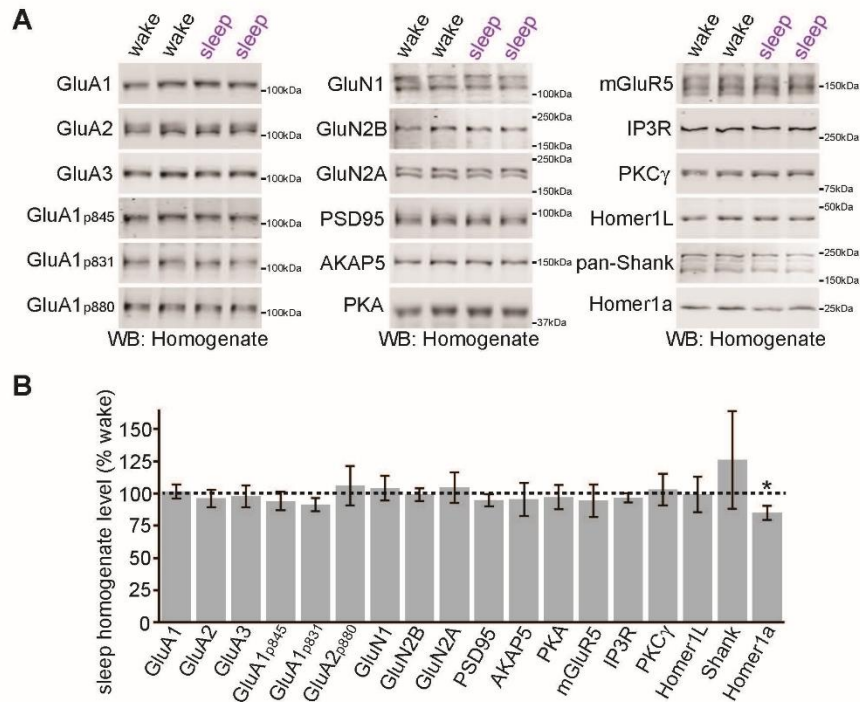


**Fig S1. Wake/sleep forebrain protein expression.** **A, B,** Western blot analysis of wake/sleep forebrain homogenate.  $N = 8$  for each condition,  $*P < 0.05$ , Student's t-test. Total Homer1a protein expression was significantly reduced during sleep compared to wake. No other proteins showed significant changes in total protein expression, suggesting that changes that occur in synaptic fractions reflect protein trafficking to and from synapses and not overall changes in protein expression. Quantification indicate mean  $\pm$  SEM.

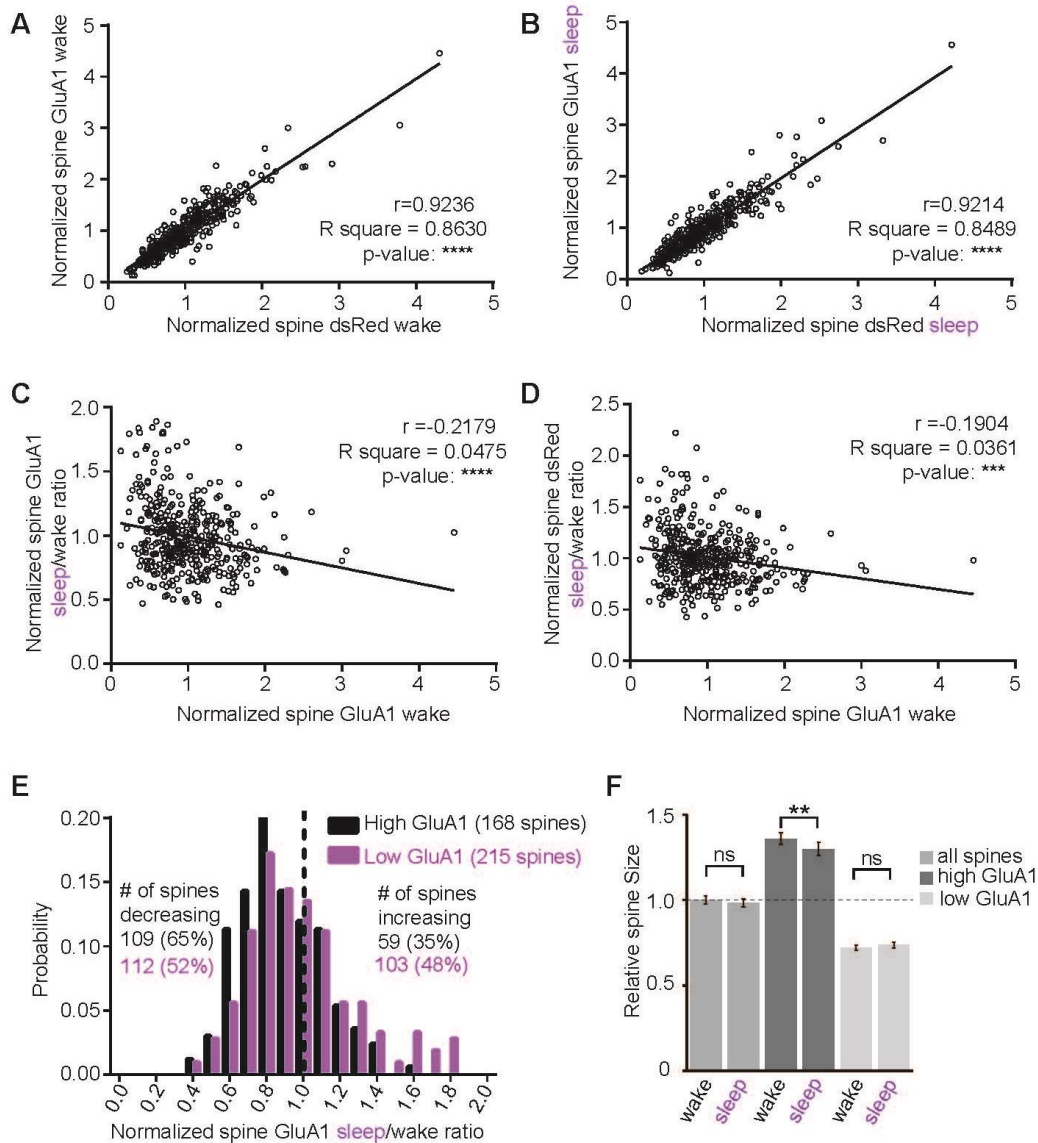


**Fig. S2. Spines with greater GluA1 abundance are disproportionately weakened during sleep.** **A, B**, Normalized spine GluA1 values are highly correlated with spine size (normalized spine dsRed) during wake (**A**) and sleep (**B**). **C, D**, Correlation between spine GluA1 in the wake phase and the change in spine GluA1 during sleep (spine GluA1 sleep/wake ratio) (**C**) or spine dsRed sleep/wake ratio (**D**). Negative slope indicates spines with greater GluA1 levels in the wake phase are more likely to lose GluA1 (**C**) and shrink in size (**D**) during sleep. **E**, Change in spine GluA1 (sleep/wake ratio) histogram. Spines were grouped into high and low GluA1 (greater or less than average spine GluA1 in the wake phase). Spines with high GluA1 show a greater degree of reduction in spine GluA1 during sleep, significantly different from a randomized distribution, Kolmogorov-Smirnov test,  $P < 0.01$ . Spines with low GluA1 are unaffected. “high GluA1”  $N = 168$  spines, “low GluA1”  $N = 215$  spines, from 4 mice. High GluA1 distribution significantly different from low GluA1 distribution, Kolmogorov-Smirnov test,  $P < 0.05$ . **F**, Relative spine size is significantly reduced during sleep compared to wake for spines with high GluA1.  $N = 383$  spines from 4 mice, “high GluA1”  $N = 168$  spines, “low GluA1”  $N =$

215 spines, \*\*P < 0.01, ns = not significant Student's t-test. Quantification indicate mean  $\pm$  SEM.

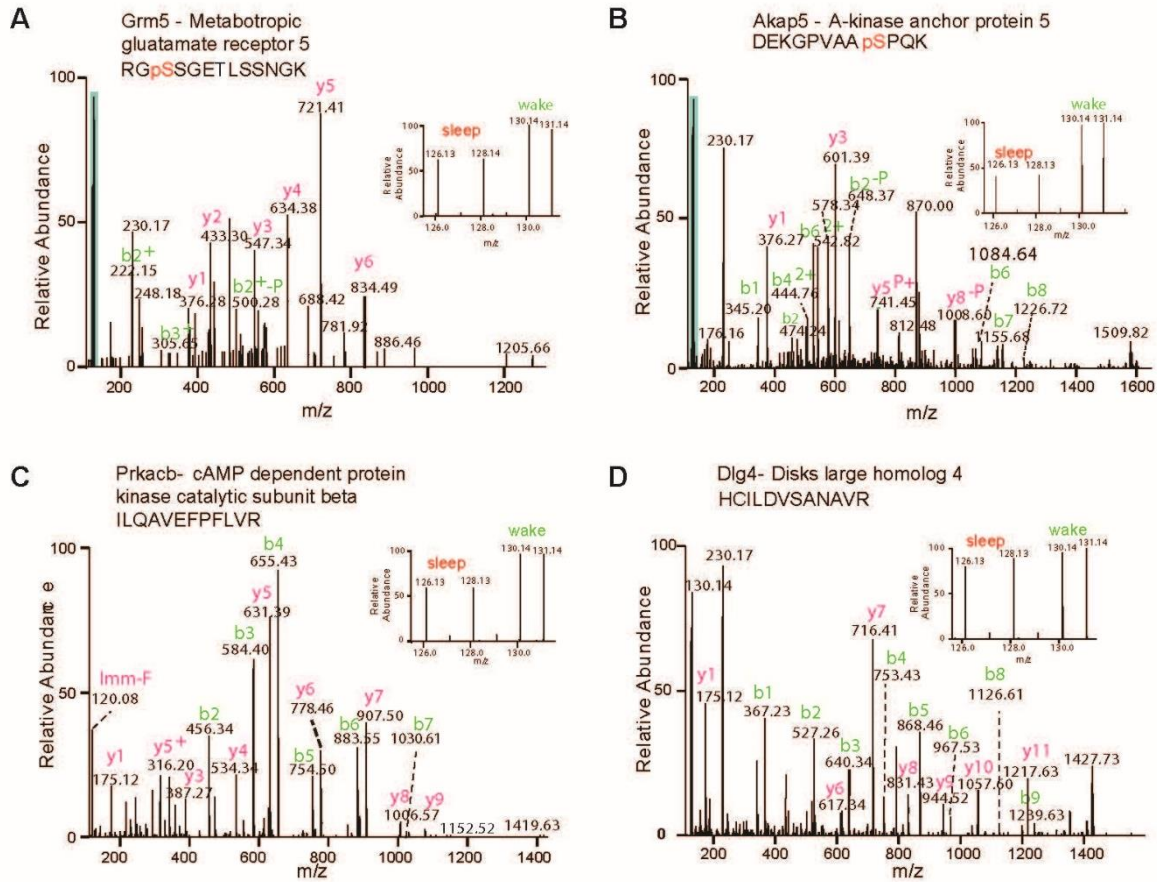


**Fig. S3. Quantitative proteomics of wake/sleep changes in PSD.** Forebrain (Cortex plus hippocampus) PSD samples were prepared during the wake (10pm) or sleep (10am) phase followed by quantitative proteomics using the tandem mass tag (TMT) method. Sample mass spectrometry spectra from wake/sleep PSD samples: **A**, Grm5 (mGluR5 alpha isoform) phospho-S870. **B**, AKAP5 phospho-S29. **C**, Prkacb (PKA catalytic subunit beta). **D**, Dlg4 (PSD95). The identified peptide sequences are shown, phosphorylated residues are highlighted in red. Inset shows the TMT signals used for quantification.

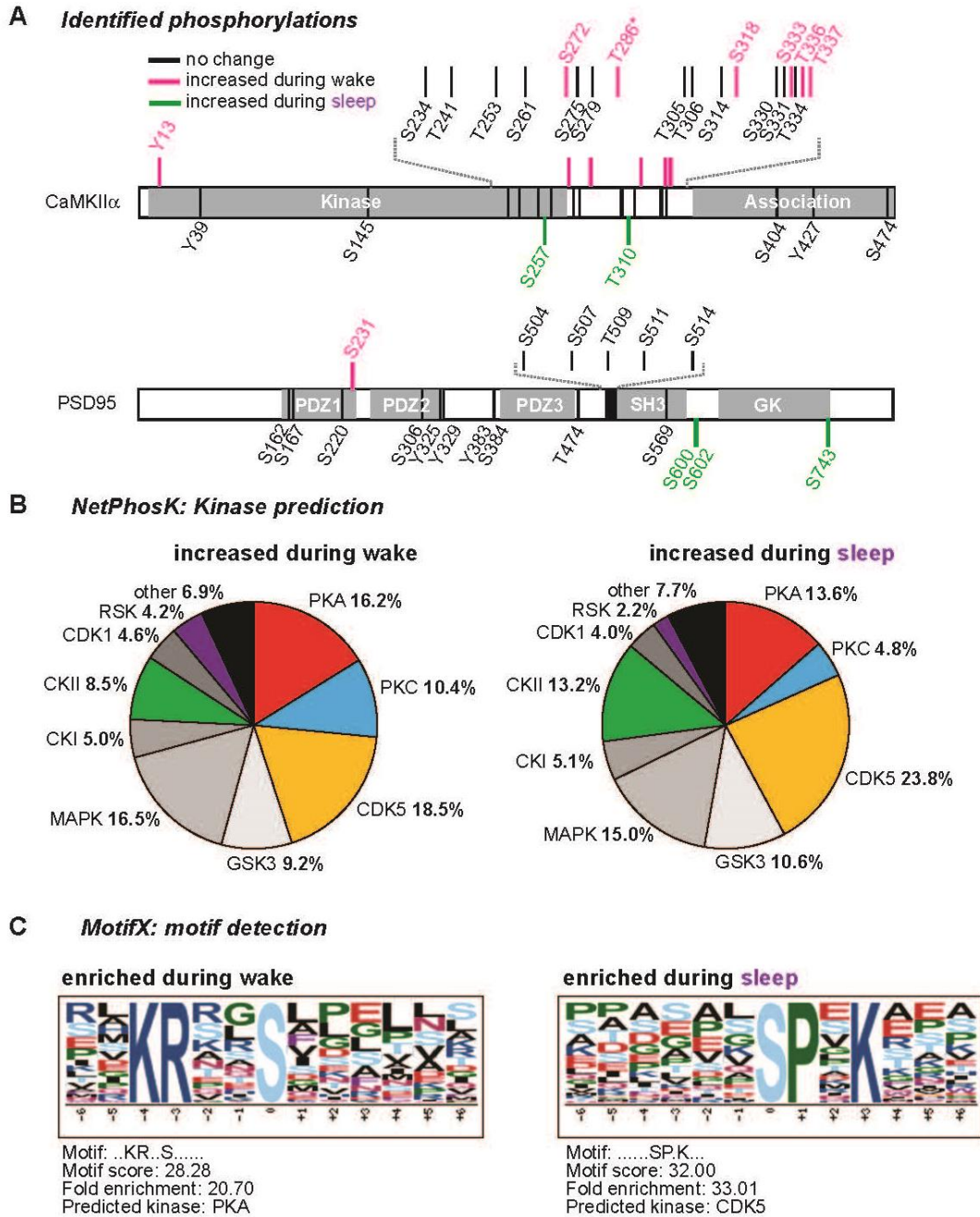


**Fig. S4. Wake/sleep phase regulation of kinase activity in PSD.** **A**, Phosphorylation sites identified by mass-spectrometry for CaMKII $\alpha$  and PSD95 as examples of the wake/sleep phospho-proteome. Both proteins contain phosphorylations that were not changed or increased during wake or sleep respectively. The activation site of CaMKII $\alpha$  is indicated by an asterisk, protein domains are indicated in grey. **B**, A web-based kinase prediction program (<http://www.cbs.dtu.dk/services/NetPhosK>) was used to predict the responsible kinase for the 500 most highly regulated PSD phospho-peptides identified using phospho-proteomics (250 phosphorylations increased during wake and 250 phosphorylations increased during sleep, see supplementary tables). Phospho-peptides predicted to be targeted by the indicated kinases are presented as a percentage of the total

number of phospho-sites analyzed for each group. Kinase prediction suggests that during wake, more peptides are phosphorylated by PKA and PKC, while during sleep more peptides are phosphorylated by CDK5 or CKII. C, Motif-X ([motif-x.med.harvard.edu](http://motif-x.med.harvard.edu)) analysis (31) was used to detect enriched phosphorylation motifs in identified PSD phosphorylations increased during wake (1181 phosphorylations) or sleep (790 phosphorylations)(see supplementary tables). The most highly enriched motifs for wake or sleep are shown, and correspond to consensus targets for PKA and CDK5 respectively. These analysis suggest that during wake (10pm) PKA is more active at synapses, while during sleep (10am) CDK5 is more active at synapses.

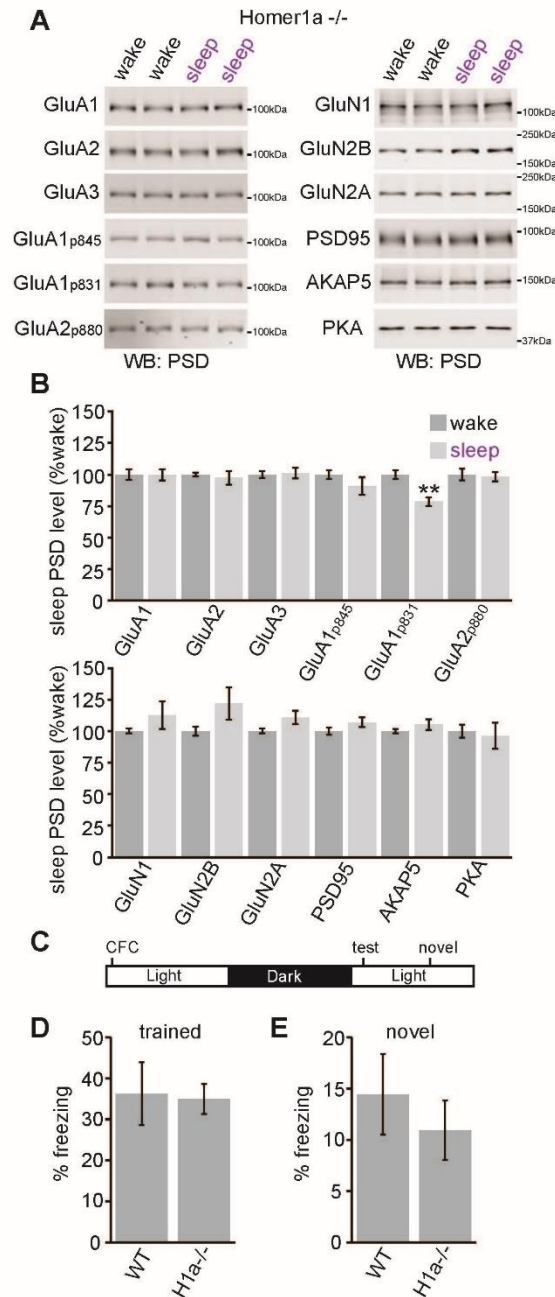


**Fig. S5. Wake/sleep PSD analysis and contextual fear memory in Homer1a knock-out mice.** **A, B**, Western blot analysis of wake/sleep PSD fractions from Homer1a knock-out mice.  $N = 8$  brains for each condition,  $**P < 0.01$ , Student's  $t$ -test. Changes seen in wake/sleep PSD in wild-type mice are absent from Homer1a knock-out mice, with the exception of changes in phosphorylation of GluA1<sub>S831</sub>, which we conclude is Homer1a independent. **C-E**, Homer1a knock-out and wild-type littermates were trained in contextual fear conditioning at the beginning of the sleep phase. Mice were tested 24hrs later for freezing responses in the trained context (**D**), or a novel context (**E**)  $N = 8$  WT, 14 H1a KO littermates,  $P > 0.05$  Student's  $t$ -test. Quantification indicate mean  $\pm$  SEM.

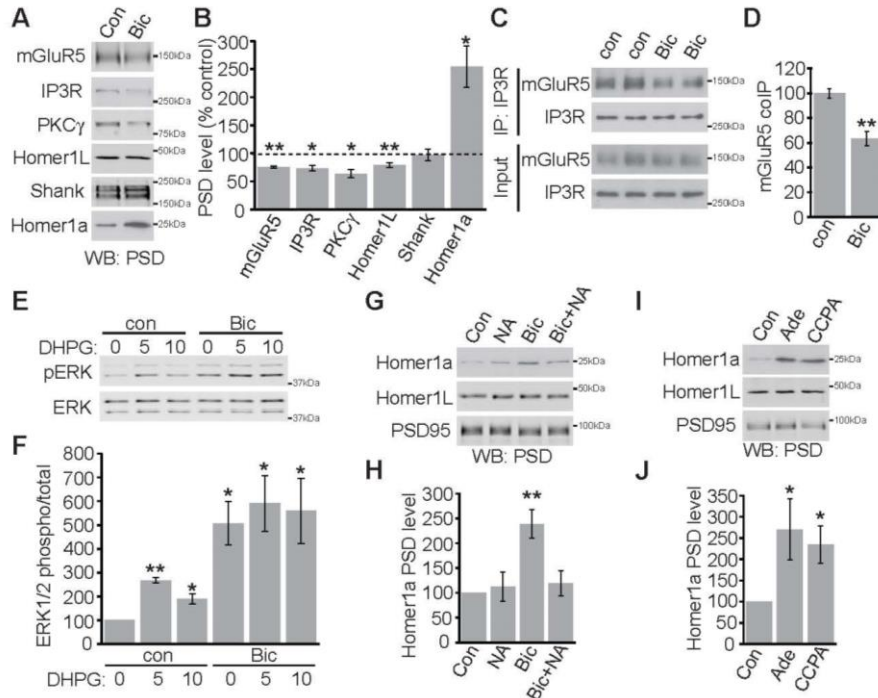


**Fig. S6. Remodeling of the mGluR5 signaling complex during homeostatic scaling-down.** **A, B**, Western blot analysis of PSD fractions collected from cultured cortical neurons (13-14DIV) treated with or without bicuculline (20μM) for 24hrs. N = 5, \*P < 0.05, \*\*P < 0.01, Student's t-test. **C, D**, Co-immunoprecipitation of mGluR5 and IP3R in bicuculline treated (20μM, 24hrs) cultured cortical neurons (13-14DIV). N = 6, \*\*P < 0.01 Student's t-test. **E, F**, Bicuculline pre-treatment (20μM for 24hrs) occludes activation of phospho-ERK1/2 by DHPG (100μM for 5-10min). N = 5, \*P < 0.05, \*\*P < 0.01 Student's t-test. **G, H**, Cultured cortical neurons (13-14DIV) were treated with bicuculline for 24hrs to induce targeting of Homer1a to the PSD followed by acute noradrenaline treatment (NA, 5μM for 1hr) and PSD prep. Acute NA treatment is able to reverse PSD targeting of Homer1a induced by bicuculline. N = 6, \*\*P < 0.01 Student's t-test. **I, J**, Cultured cortical neurons (13-14DIV) were treated with adenosine (Ade, 10μM) or adenosine A1 receptor agonist CCPA (100nM) for 30min followed by PSD prep. Adenosine or CCPA caused recruitment of Homer1a into the PSD. N = 4, \*P < 0.05, Student's t-test. Quantification indicate mean ± SEM.



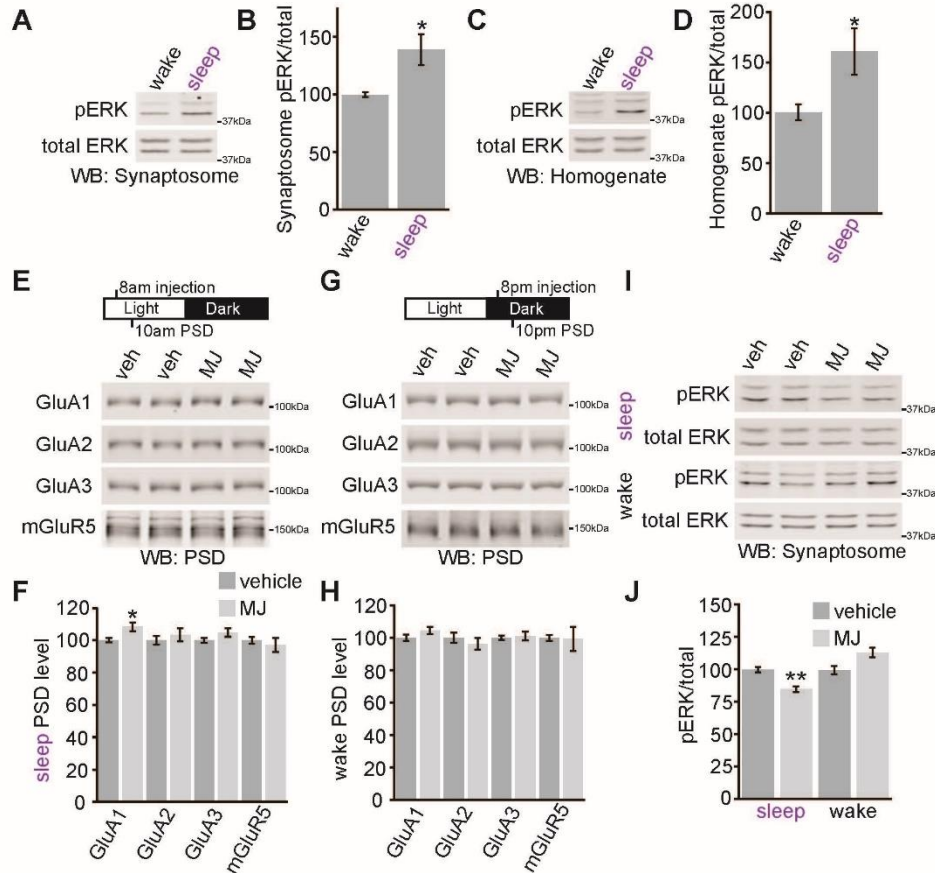


**Fig. S7. ERK1/2 activity is increased during the sleep phase and mGluR1/5 activity drives scaling-down during the sleep phase.** A-D, forebrains were isolated during the wake or sleep phase followed by homogenization and sub-cellular fractionation to isolate synaptosomes. Phosphorylated and total ERK1/2 were detected in synaptosomes (A) or homogenate (C). Phospho/total ERK1/2 is significantly increased in synaptosomes (B) or homogenate (D) during sleep compared wake. N = 10, \*P < 0.05 Student's t-test. E-J, Mice were injected with vehicle or MTEP/JNJ (5mg/kg/2.5mg/kg, MJ) and 2hrs later at 10am (E, F) or 10pm (G, H) PSD fractions were prepared. MJ caused a significant increase in GluA1 in the PSD during the sleep, but not the wake phase. MJ caused a significant decrease in phospho-ERK1/2 during sleep but not wake (I, J). N = 7 for each condition, \*P < 0.05, \*\*P < 0.01 Student's t-test. Quantification indicate mean  $\pm$  SEM.

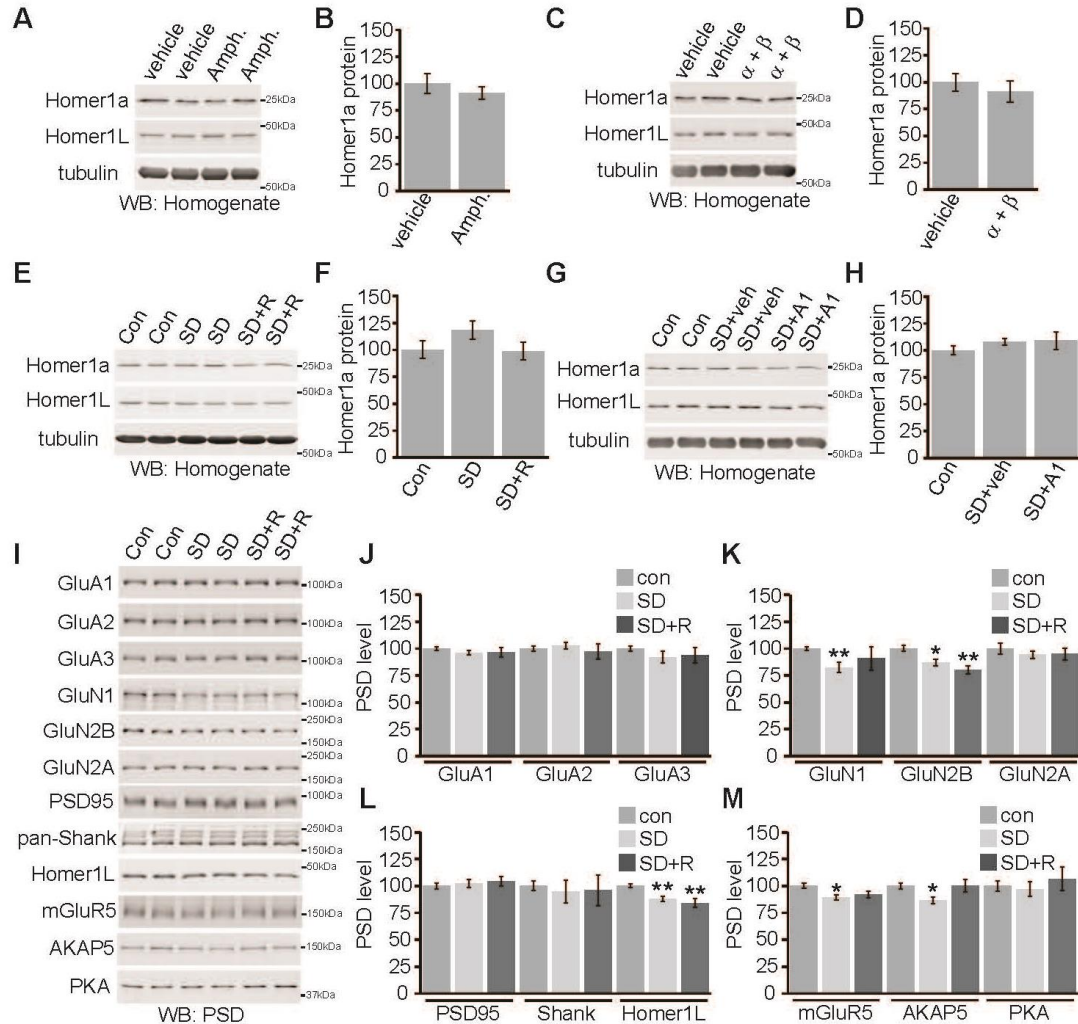


**Fig. S8. Total Homer1a protein and changes in PSD proteins during sleep deprivation.** A-H, Experimental treatments did not result in significant changes in total forebrain homogenate levels of Homer1a protein. A, B, Mice were injected with D-amphetamine (Amph., 2mg/kg) at 8am and forebrain homogenate was prepared 2hrs later at 10am. N = 5. C, D, Mice were injected with prazosin ( $\alpha$ , 2mg/kg) and propranolol ( $\beta$ , 20mg/kg) at 8pm and forebrain homogenate was prepared 2hrs later at 10pm. N = 4. E, F, Mice were sleep deprived (SD) for 4hrs (6-10am) by placing mice into a new cage with or without recovery sleep (2.5hrs, SD+R) in their original cage, followed by forebrain homogenate prep. N = 8. G, H, Mice were left in their home cage (con) or subjected to 4hrs SD (6-10am) with two injections spaced 2hrs apart of vehicle or adenosine A1 receptor inhibitor DPCPX (A1, 0.5mg/kg). N = 6. I-M, Mice were sleep deprived (SD) for 4hrs (6-10am) by placing mice into a new cage with or without recovery sleep (2.5hrs, SD+R) in their original cage, followed by forebrain PSD prep. SD resulted in a significant decrease in PSD-associated GluN1/GluN2B NMDAR subunits, Homer1L, mGluR5 and AKAP5. N = 8, \*P < 0.05, \*\*P < 0.01 Student's t-test with Bonferroni correction. Quantification indicate mean  $\pm$  SEM.

**Table S1.**

Proteins enriched in the PSD during the wake/sleep phase (10pm/10am). **A**, Proteins enriched in the PSD during wake (10pm/10am ratio > 1.3). **B**, Proteins enriched in the PSD during sleep (10am/10pm ratio >1.3, or 10pm/10am ratio < 0.77).

**Table S2.**

Phosphorylation sites hyper-phosphorylated during the wake/sleep phase (10pm/10am). **A**, Phosphorylations hyper-phosphorylated in the PSD during wake (10pm/10am ratio > 1.3). **B**, Phosphorylations hyper-phosphorylated in the PSD during sleep (10am/10pm ratio >1.3, or 10pm/10am ratio < 0.77).

## References and Notes

1. S. Diekelmann, J. Born, The memory function of sleep. *Nature reviews. Neuroscience* **11**, 114-126 (2010).
2. C. G. Vecsey *et al.*, Sleep deprivation impairs cAMP signalling in the hippocampus. *Nature* **461**, 1122-1125 (2009).
3. V. V. Vyazovskiy, C. Cirelli, M. Pfister-Genskow, U. Faraguna, G. Tononi, Molecular and electrophysiological evidence for net synaptic potentiation in wake and depression in sleep. *Nature neuroscience* **11**, 200-208 (2008).
4. Z. W. Liu, U. Faraguna, C. Cirelli, G. Tononi, X. B. Gao, Direct evidence for wake-related increases and sleep-related decreases in synaptic strength in rodent cortex. *The Journal of neuroscience : the official journal of the Society for Neuroscience* **30**, 8671-8675 (2010).
5. G. Tononi, C. Cirelli, Sleep and the price of plasticity: from synaptic and cellular homeostasis to memory consolidation and integration. *Neuron* **81**, 12-34 (2014).
6. G. G. Turrigiano, The self-tuning neuron: synaptic scaling of excitatory synapses. *Cell* **135**, 422-435 (2008).
7. A. Goel, H. K. Lee, Persistence of experience-induced homeostatic synaptic plasticity through adulthood in superficial layers of mouse visual cortex. *The Journal of neuroscience : the official journal of the Society for Neuroscience* **27**, 6692-6700 (2007).
8. K. B. Hengen, A. Torrado Pacheco, J. N. McGregor, S. D. Van Hooser, G. G. Turrigiano, Neuronal Firing Rate Homeostasis Is Inhibited by Sleep and Promoted by Wake. *Cell* **165**, 180-191 (2016).
9. G. H. Diering, A. S. Gustina, R. L. Huganir, PKA-GluA1 Coupling via AKAP5 Controls AMPA Receptor Phosphorylation and Cell-Surface Targeting during Bidirectional Homeostatic Plasticity. *Neuron* **84**, 790-805 (2014).
10. J. H. Hu *et al.*, Homeostatic scaling requires group I mGluR activation mediated by Homer1a. *Neuron* **68**, 1128-1142 (2010).
11. R. J. O'Brien *et al.*, Activity-dependent modulation of synaptic AMPA receptor accumulation. *Neuron* **21**, 1067-1078 (1998).
12. R. L. Huganir, R. A. Nicoll, AMPARs and synaptic plasticity: the last 25 years. *Neuron* **80**, 704-717 (2013).
13. Y. Zhang, R. H. Cudmore, D. T. Lin, D. J. Linden, R. L. Huganir, Visualization of NMDA receptor-dependent AMPA receptor synaptic plasticity in vivo. *Nature neuroscience* **18**, 402-407 (2015).
14. J. C. Tu *et al.*, Homer binds a novel proline-rich motif and links group 1 metabotropic glutamate receptors with IP3 receptors. *Neuron* **21**, 717-726 (1998).
15. P. R. Brakeman *et al.*, Homer: a protein that selectively binds metabotropic glutamate receptors. *Nature* **386**, 284-288 (1997).
16. N. Naidoo *et al.*, Role of Homer proteins in the maintenance of sleep-wake states. *PLoS one* **7**, e35174 (2012).
17. A. Ahnaou, X. Langlois, T. Steckler, J. M. Bartolome-Nebreda, W. H. Drinkenburg, Negative versus positive allosteric modulation of metabotropic glutamate receptors (mGluR5): indices for potential pro-cognitive drug properties based on EEG network oscillations and sleep-wake organization in rats. *Psychopharmacology*, (2014).
18. A. Ahnaou, L. Raeymaekers, T. Steckler, W. H. Drinkenburg, Relevance of the metabotropic glutamate receptor (mGluR5) in the regulation of NREM-REM sleep cycle and homeostasis: evidence from mGluR5 (-/-) mice. *Behavioural brain research* **282**, 218-226 (2015).

19. S. Maret *et al.*, Homer1a is a core brain molecular correlate of sleep loss. *Proceedings of the National Academy of Sciences of the United States of America* **104**, 20090-20095 (2007).
20. M. Mackiewicz, B. Paigen, N. Naidoo, A. I. Pack, Analysis of the QTL for sleep homeostasis in mice: Homer1a is a likely candidate. *Physiological genomics* **33**, 91-99 (2008).
21. J. C. Tu *et al.*, Coupling of mGluR/Homer and PSD-95 complexes by the Shank family of postsynaptic density proteins. *Neuron* **23**, 583-592 (1999).
22. F. Ango *et al.*, Agonist-independent activation of metabotropic glutamate receptors by the intracellular protein Homer. *Nature* **411**, 962-965 (2001).
23. K. L. Eckel-Mahan *et al.*, Circadian oscillation of hippocampal MAPK activity and cAmp: implications for memory persistence. *Nature neuroscience* **11**, 1074-1082 (2008).
24. S. Thandi, J. L. Blank, R. A. Challiss, Group-I metabotropic glutamate receptors, mGlu1a and mGlu5a, couple to extracellular signal-regulated kinase (ERK) activation via distinct, but overlapping, signalling pathways. *Journal of neurochemistry* **83**, 1139-1153 (2002).
25. D. Chaudhury, C. S. Colwell, Circadian modulation of learning and memory in fear-conditioned mice. *Behavioural brain research* **133**, 95-108 (2002).
26. G. Aston-Jones, F. E. Bloom, Activity of norepinephrine-containing locus coeruleus neurons in behaving rats anticipates fluctuations in the sleep-waking cycle. *The Journal of neuroscience : the official journal of the Society for Neuroscience* **1**, 876-886 (1981).
27. T. E. Bjorness *et al.*, An Adenosine-Mediated Glial-Neuronal Circuit for Homeostatic Sleep. *The Journal of neuroscience : the official journal of the Society for Neuroscience* **36**, 3709-3721 (2016).
28. Z. Chen *et al.*, Prolonged adenosine A1 receptor activation in hypoxia and pial vessel disruption focal cortical ischemia facilitates clathrin-mediated AMPA receptor endocytosis and long-lasting synaptic inhibition in rat hippocampal CA3-CA1 synapses: differential regulation of GluA2 and GluA1 subunits by p38 MAPK and JNK. *The Journal of neuroscience : the official journal of the Society for Neuroscience* **34**, 9621-9643 (2014).
29. T. Serchov *et al.*, Increased Signaling via Adenosine A1 Receptors, Sleep Deprivation, Imipramine, and Ketamine Inhibit Depressive-like Behavior via Induction of Homer1a. *Neuron* **87**, 549-562 (2015).
30. B. O. Watson, D. Levenstein, J. P. Greene, J. N. Gelinis, G. Buzsaki, Network Homeostasis and State Dynamics of Neocortical Sleep. *Neuron* **90**, 839-852 (2016).
31. D. Schwartz, M. F. Chou, G. M. Church, Predicting protein post-translational modifications using meta-analysis of proteome scale data sets. *Mol Cell Proteomics* **8**, 365-379 (2009).
32. T. Saito, N. Nakatsuji, Efficient gene transfer into the embryonic mouse brain using in vivo electroporation. *Dev Biol* **240**, 237-246 (2001).
33. T. A. Pologruto, B. L. Sabatini, K. Svoboda, ScanImage: flexible software for operating laser scanning microscopes. *Biomed Eng Online* **2**, 13 (2003).
34. M. S. Kim *et al.*, A draft map of the human proteome. *Nature* **509**, 575-581 (2014).
35. J. V. Olsen *et al.*, Parts per million mass accuracy on an Orbitrap mass spectrometer via lock mass injection into a C-trap. *Mol Cell Proteomics* **4**, 2010-2021 (2005).